History:
Received: May 12, 2024
Revised: May 21, 2024
Accepted: June 7, 2024
Published: June 11, 2024
Collection year: 2024
Status: Published

Identifiers and Pagination:
Year: 2024
Volume: 9
First Page: 1
Last Page: 22
Publisher ID: 10.21065/ AdvBioScie.9.1
doi:http://dx.doi.org/10.21065/AdvBioScie.9.1

Corresponding author:
Amani A. Abdelghani & **Marya Ahmed** Department of Chemistry, University of Prince Edward Island, 550 University Avenue, Charlottetown, PE, C1A 4P3, Canada.
E.: aabdelghani@upei.ca & marahmed@upei.ca

Citation:
Marcus J. Gauthier, Rahimeh Rasouli, Marya Ahmed *et al.* A study on the synthesis, characterization, and biological activity of metallodendrimers drug conjugates. Adv J Biom Sci, 2024. Vol 9, p 1-22 http://dx.doi.org/10.21065/AdvBioScie.9.1

Funding:
The authors received no direct funding for this research.

Competing Interests:
The authors declare no competing interests

Additional information is available at the end of the article.

Original Research Article

A STUDY ON THE SYNTHESIS, CHARACTERIZATION, AND BIOLOGICAL ACTIVITY OF METALLODENDRIMERS DRUG CONJUGATES

Marcus J. Gauthier,[a] Rahimeh Rasouli,[a] Marya Ahmed,*[a] and Amani A. Abdelghani,*[a,b]

a) *Department of Chemistry, University of Prince Edward Island, 550 University Avenue, Charlottetown, PE, C1A 4P3, Canada.*
b) *Chemistry Department, Faculty of Science, Damanhour University, Damanhour 22511, Beheira, Egypt.*

Abstract:

This study reports the synthesis and characterization of metallodendrimers that incorporate anti-inflammatory drugs and evaluates their anti-inflammatory and antimicrobial properties. The inclusion of cationic cyclopentadienyliron moieties contributed to these positive biological activity outcomes. The safety of the dendrimers was assessed using *in vitro* toxicity tests on mammalian cell lines, and it was revealed that the dendrimers connected to the drugs were less toxic compared to the others. Among the best dendrimers, second-generation dendrimer with OH end groups (D7-G2-OH) and first-generation dendrimer with indomethacin end groups (D5-G1-I) showed promising antimicrobial properties. The chemical structure of the dendrimers was analyzed using FT-IR, ^{1}H-NMR, and ^{13}C-NMR spectroscopy, providing information about the functional groups and bonding patterns present. Thermal stability was assessed using thermogravimetric analysis (TGA) and showed exceptional stability of dendrimers within the temperature range of 300-400 °C. However, the cationic iron moieties in the dendrimers underwent breakdown at approximately 200 °C. Scanning electron micrographs (SEM) revealed that the morphology of the dendrimers varied across different generations, indicating structural changes as the dendrimer size increased. Furthermore, cyclic voltammetry analysis (CV) demonstrated changes in the intensity and broadness of the redox waves as the dendrimer generation increased, suggesting alterations in the electrochemical behavior of the dendrimers.

Keywords: Sulindac, indomethacin, gram-positive strain, gram-negative strain, anti-inflammatory, Thermogravimetric, CV, Scanning electron micrographs.

1. INTRODUCTION

Over the past decades, the field of nanomedicine has experienced significant progress and has found applications in drug delivery, imaging, diagnostics, tissue engineering, cancer treatment, and theragnostic.[1-3]

Dendrimers are a significant class of nanoscale polymeric molecules that have shown great potential in nanomedicine, particularly in drug delivery applications.[4,5] Dendrimers have branching structures with a central core that allows for precise control over the size, shape, and surface functionality of the dendrimer nanoparticles.[4,5] These attributes of dendrimers show continuing promise in the safety and efficiency of being used as drug carriers for numerous treatments of parasitic, viral, and bacterial infections.[6] Dendrimers can encapsulate drug molecules within their interior void spaces, branches, or on the surface and can be engineered to release drugs in a controlled manner.[7-9] Dendrimers can also be functionalized with imaging agents, such as fluorescent dyes or contrast agents, enabling them to act as imaging probes.[10,11] Interestingly, some dendrimers possess inherent antimicrobial or anticancer activities, making them promising candidates for standalone therapies.[12,13] In addition, the surface of dendrimers can be modified with specific targeting ligands, such as antibodies or peptides, which enables selective binding to specific cells or tissues.[7,14-17] This targeted delivery approach improves drug concentration at the desired site, minimizing off-target effects and reducing systemic toxicity.

Furthermore, the inclusion of metal compounds in the dendritic structure leads to the development of other useful properties.[18-24] For example, magnetic properties arise due to the presence of metal centers within the dendrimer structure and can be exploited in various fields, including electronics, sensors, and catalysis.[25-27] Metallodendrimers can also facilitate efficient energy transfer processes, allowing for applications in areas such as light harvesting and photovoltaics.[28-31] Recently, metallodendrimers have also gained interest in the field of biology due to their unique properties and potential applications in various biological studies.[5,32,33] Metallodendrimers have the capability to mitigate the toxicity associated with oral ingestion by enabling a more regulated drug release.[34,35] They serve as a carrier mechanism for bonding molecules, including commonly used drugs, to the multiple branches of the nanoparticles.

Nonsteroidal anti-inflammatory drugs (NSAIDs), a widely used drug family, can be easily attached to these dendrimer branches.[36-39] Our previous research has shown successful synthesis of ibuprofen, ketoprofen, mefenamic acid, and aspirin conjugated dendrimers.[34,35,40] The findings from these studies support the need for additional investigation into the potential of attaching various drugs to dendrimer branches. This paper will address the potential for attaching two additional NSAIDs, sulindac and indomethacin, to dendrimers. Both sulindac and indomethacin are NSAIDs that are commonly used to reduce inflammation and relieve pain.[41-43] They belong to the same class of NSAIDs as ibuprofen, ketoprofen, and mefenamic acid, and exert their effects through the inhibition of cyclooxygenase (COX) enzymes.[44-47] Sulindac and indomethacin work by inhibiting the activity of the COX enzymes, specifically COX-1 and COX-2. These enzymes play a crucial role in the production of prostaglandins, which are lipid autacoids involved in promoting inflammation, pain, and fever. They are primarily used in the treatment of inflammatory conditions, including rheumatoid arthritis, osteoarthritis, and ankylosing spondylitis. It is also sometimes prescribed for acute pain and gout.[42] Sulindac and indomethacin help to alleviate pain, reduce inflammation, and improve joint function. The most common side effects may include gastrointestinal symptoms such as stomach upset, heartburn, nausea, and diarrhea.[48,49] An interesting point about the use of sulindac is that recent studies have shown promising anti-cancer properties.[41,50] Several studies state, a potent immune modulator, sulindac might be used to design novel tumor immunotherapy strategies.

This paper focuses on the synthesis of six new dendrimers across three generations with attached sulindac and indomethacin at the peripheries. Spectroscopic tools will be employed to evaluate the structures of these dendrimers. Other techniques, such as SEM, CV, and TGA, will also be utilized to determine their unique properties. The biological activity of synthetic dendrimers and their associated drug

conjugate will be examined to gain valuable insights into their effectiveness for potential biological applications.

2. EXPERIMENTAL

2.1 Materials

Sulindac, indomethacin, and various chemicals and reagents were purchased from Sigma Aldrich and used without further purification. The solvents used in the experiments were dried and kept over 3 Å molecular sieves before use. *Escherichia coli* (*E. coli*) ATCC 25922, a gram-negative strain, *Micrococcus Luteus* (*M. luteus*) ATCC, a gram-positive strain, and Raw 264.7 cells, a mouse macrophage cell line, were acquired from Cedarlane (ON, Canada). Fetal bovine serum (FBS) and Dulbecco's modified eagle medium/nutrient mixture F-12 (DMEM/F-12), were purchased from Fisher Scientific (ON, Canada). CellTiter 96® AQueous Cell Proliferation Assay kit was purchased from Promega (Madison, WI, USA). Lipopolysaccharide (LPS) was obtained from Sigma-Aldrich.

2.2 Instrumentation

All synthesized complexes were characterized using a Bruker Avance NMR spectrometer (1H, 300 MHz and 13C, 75 MHz) in DMSO-d6, with the chemical signals referenced to the solvent residual signal in ppm. A Bruker Alpha-P FTIR spectrometer conducted measurements for attenuated total reflection Fourier transform IR (FTIR) absorption spectroscopy. Cyclic voltammetric experiments were carried out using a Princeton Applied Research/EG&G Model 263 potentiostat/galvanostat with a glassy carbon working electrode, Pt counter electrode, and Ag reference electrode. The experiments were conducted at a scan rate of 0.1 to 2.0 V/s and 0°C in an atmosphere of nitrogen in degassed propylene carbonate, using tetrabutylammonium hexafluorophosphate (Bu4NPF6) as the supporting electrolyte and referencing to the dimethylformamide (DMF) solution of ferrocene. Scanning electron micrographs (SEM) of the prepared dendrimers were captured using a Hitachi SEM. Thermogravimetric analysis (TGA) was performed in platinum pans under nitrogen at a heating rate of 10°C using a TA Instruments TGA.

The dendrimers' hydrodynamic size and ζ-potential were measured by Brookhaven's NanoBrook 90Plus PALS instrument (American Brookhaven NanoBrook Omni).

2.3 Synthesis and Characterization

To create the six drug-modified dendrimers, the Steglich esterification method was utilized.[51] The specific molar ratios of the dendrimer core and the drugs were used in the synthesis. The 1st generation dendrimer four is connected to sulindac (D4-G1-S), the 1st generation dendrimer five is linked to indomethacin (D5-G1-I), the 2nd generation dendrimer eight is attached to sulindac (D8-G2-S), the 2nd generation dendrimer nine is connected to indomethacin (D9-G2-I), the 3rd generation dendrimer 12 is attached to sulindac (D12-G3-S), and the 3rd generation dendrimer 13 is linked to indomethacin (D13-G3-I). The reaction involved the use of the catalysts DCC (dicyclohexylcarbodiimide) and DMAP (4-dimethylaminopyridine) to form the ester linkage between the carboxylic acid groups of sulindac and indomethacin drugs and the hydroxyl groups of the 4-hydroxybenzyl alcohol. During the synthesis, the reaction mixture was agitated at 0°C under a nitrogen atmosphere for 10 minutes and then at room temperature for 48 hours. Following removing impurities through filtration, the mixture was introduced to a 10% HCl solution and filtered once more. The resulting crude products were dissolved in acetone and chilled to eliminate impurities. Finally, the solvent has evaporated, yielding the final product. The dendrimers produced were subject to analysis using ^{1}H and ^{13}C NMR spectroscopy, ATR-FTIR, and various other physical characterization methods. Further details concerning the synthetic process, molecular weight, yield percentages, and physical characterization data are provided below. All organoiron complexes used to construct dendrimer branches were synthesized using previously reported methods.[51-53] Additionally, the synthesis of the zero-generation dendrimer D1-G0-COOH, first-generation

dendrimers D2-G1-Cl, D3-G1-OH, second-generation dendrimers D6-G2-Cl, D7-G2-OH, and third-generation dendrimers D10-G3-Cl, D11-G3-OH was carried out using established methods.[53]

Synthesizing and Characterizing the Dendrimers Functionalized with a Novel Drug

2.3.1 Sulindac-terminal dendrimer (D4-G1-S)

To synthesize D4-G1-S, an esterification reaction was carried out using sulindac and dendrimer D3-G1OH. The process involved placing D3-G1-OH (0.500 g, 0.065 mmol), sulindac (0.185 g, 0.052 mmol), and DMAP (0.063 g, 0.052 mmol) in a 25 mL round-bottom flask. The mixture was dissolved in 10 mL of DMF and put in an ice bath for 10 minutes with gentle stirring. DCC (0.110 g, 0.052 mmol) was slowly added to the mixture over 5 minutes, after which it was stirred under nitrogen at room temperature for 10 minutes and then allowed to stand for 48 hours. The resulting product was added to 300 mL of 10% HCl solution, then NH_4PF_6 (0.085 g, 0.052 mmol) to induce complete precipitation. The product's molecular weight is 10407 g/mol, yielding 73%. ATR-FTIR; n_{max}/cm^{-1}: 2933 (Ar-CH), 2897 (Cp-CH), 1712 (CO), 1244 (C-O-C). ^{1}H NMR data d_H (300 MHz; DMSO-d_6): 7.66 (40H, s, uncompleted O-Ar-H), 7.53 (16H, m, sulindac SO-Ar-H), 7.37 (8H, s, uncomplexed CO-Ar-H), 7.34-7.31 (32H, d, *J = 8.1 Hz*, uncomplexed Ar-H), 7.29 (16H, s, sulindac-Ar-H), 7.26 (8H, m, sulindac Ar-H), 7.04 (8H, s, sulindac-Ar-H), 6.94 (8H, dd, sulindac-Ar-H), 6.73 (8H, s, complexed Ar-H), 6.27 (40H, s, complexed Ar-H), 5.33 (8H, s, sulindac-aliph-H), 5.22 (40H, s, outer Cp-H), 5.19 (20H, s, inner Cp-H), 5.06 (16H, s, benzyl-CH_2), 4.56 (8H, s, Core-O-CH_2), 4.29 (8H, s, Core-S-CH_2), 3.97 (16H, s, aliphatic-CH_2), 3.87 (16H, s, sulindac-CH_2), 3.76 (16H, s, aliphatic-CH_2), 3.73 (16H, s, aliphatic-CH_2), 3.67 (16H, s, aliphatic-CH_2), 3.17 (8H, s, aliphatic-CH_2), 2.42 (8H, s, complexed-CH_2), 2.23 (24H, s, sulindac-CH_3), 2.19 (8H, s, complexed-CH_2), 1.74 (24H, s, sulindac-CH_3), 1.66 (12H, s, complexed-CH_3), (Figure **1**). ^{13}C NMR δ_c (75 MHz; DMSO-d_6): ^{13}C NMR d_c (75 MHz; DMSO-d_6): 171.76 and 167.13 (CO), 157.87, 130.66, and 129.30 (quat-C), 132.78, 126.79, 121.01, and 105.95 (uncomplexed Ar-C), 79.90 and 76.30 (complexed Ar-C), 77.97 (Cp-C), 63.69, 38.75, 36.30, 33.58, and 31.43 (CH_2), 43.11 and 24.14 (CH_3-C), (Figure **2**), $C_{493}H_{448}O_{68}Fe_{12}P_{12}F_{80}S_{12,}$ found: %C: 60.45, and %H: 4.11, theoretically: %C: 56.90, and %H: 4.34.

2.3.2 Indomethacin-terminal dendrimer (D5-G1-I)

To create D5-G1-I, indomethacin was combined with hydroxyl-terminated in D3-G1-OH, using a Steglich esterification reaction. The process involved adding D3-G2-OH (0.500 g, 0.065 mmol), indomethacin (0.186 g, 0.052 mmol), DMAP (0.063 g, 0.052 mmol), and 10 mL of DMF into a 25 mL round-bottom flask. The solution was stirred in an ice bath, under a nitrogen atmosphere, while slowly adding DCC (0.110 g, 0.052 mmol) over a 10-minute period. The same workup procedures as D4-G1-S were followed to obtain the final product.

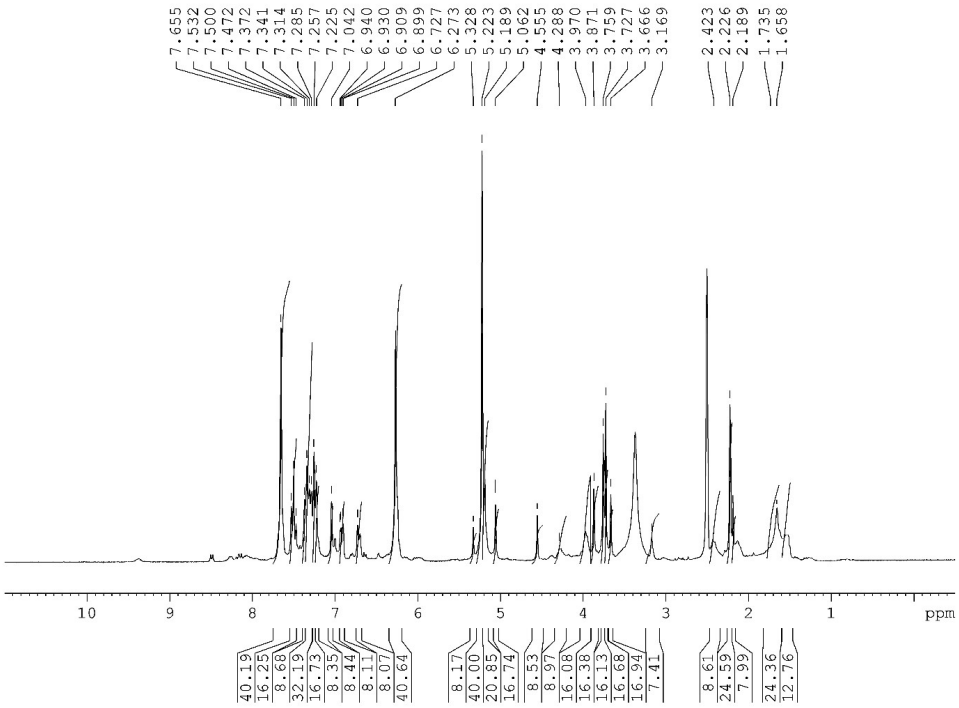

Figure 1. ^{1}H NMR spectra of **D4-G1-S** in DMSO-d_6

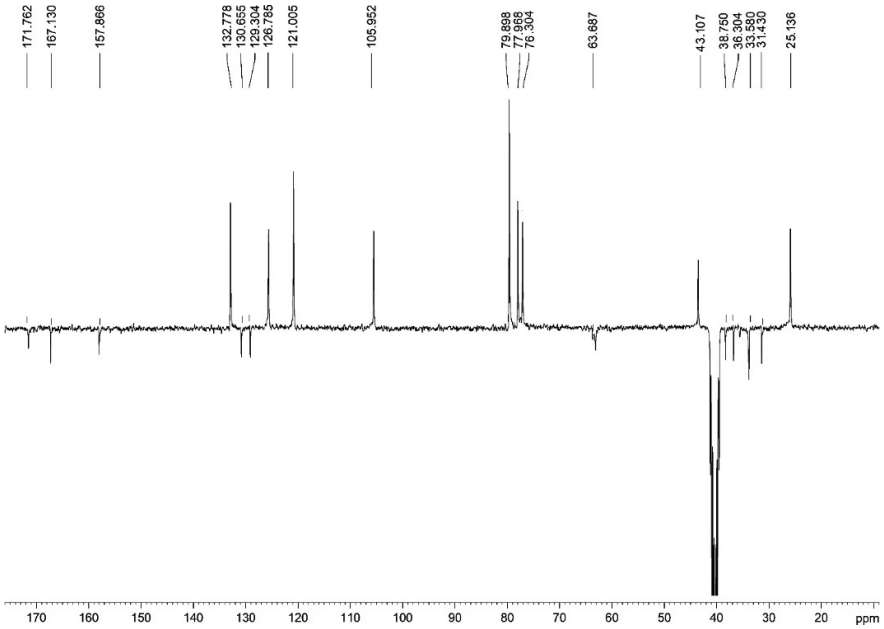

Figure 2. ^{13}C NMR spectra of **D4-G1-S** in DMSO-d_6

The product's molecular weight is 10418 g/mol, yielding 55%. ATR-FTIR; ν_{max}/cm^{-1}: 2891 (Ar-C), 2913 (Cp-C), 1706 (CO), 1220 (C-O-C). ^{1}H NMR data d_H (300 MHz; DMSO-d_6): 7.81 (16H, d, *J*

= *7.8 Hz*, indomethacin-Cl-Ar-H), 7.75 (16H, d, *J* = *8.7 Hz*, indomethacin-O-Ar-H), 7.55 (20H, s, uncompleted O-Ar-H), 7.50 (20H, s, uncompleted O-Ar-H), 7.41 (24H, m, uncomplexed CO-Ar-H + indomethacin-Ar-H), 7.36-7.34 (32H, d, *J* = *7.8 Hz*, uncomplexed Ar-H), 7.03 (8H, s, indomethacin-Ar-H), 6.74 (8H, s, complexed Ar-H), 6.27 (40H, s, complexed Ar-H), 5.22 (40H, s, outer Cp-H), 5.19 (20H, s, inner Cp-H), 5.06 (16H, s, benzyl-CH_2), 4.55 (8H, s, Core-O-CH_2), 4.26 (8H, s, Core-S-CH_2), 3.97 (16H, s, aliphatic-CH_2), 3.79 (16H, s, indomethacin-CH_2), 3.59 (16H, s, aliphatic-CH_2), 3.18 (8H, s, aliphatic-CH_2), 2.82 (32H, s, aliphatic-CH_2), 2.42 (8H, s, complexed-CH_2), 2.18 (24H, d, *J* = *4.8 Hz*, indomethacin-CH_3), 2.12 (8H, s, complexed-CH_2), 1.77 (24H, s, indomethacin-CH_3), 1.63 (12H, s, complexed-CH_3), (Figure **3**). ^{13}C NMR dc (75 MHz; DMSO-d_6): 175.49 and 170.59 (CO), 154.74, 152.15, 147.54, and 133.13, (quat-C), 142.06, 130.53, and 109.50, (uncomplexed Ar-C), 78.05 (Cp-C), 77.51 (complexed Ar-C), 45.82, 37.17, 32.85, 30.85, and 24.49 (CH_2-C), 30.833 (CH_3-C), (Figure **4)**. The Elemental Analysis of $C_{485}H_{440}O_{76}N_8Fe_{12}P_{12}F_{72}Cl_8S_4$, found: %C: 60.81, %N: 1.12, and %H: 4.09, theoretically: %C: 55.91, %N: 1.08, and %H: 4.26.

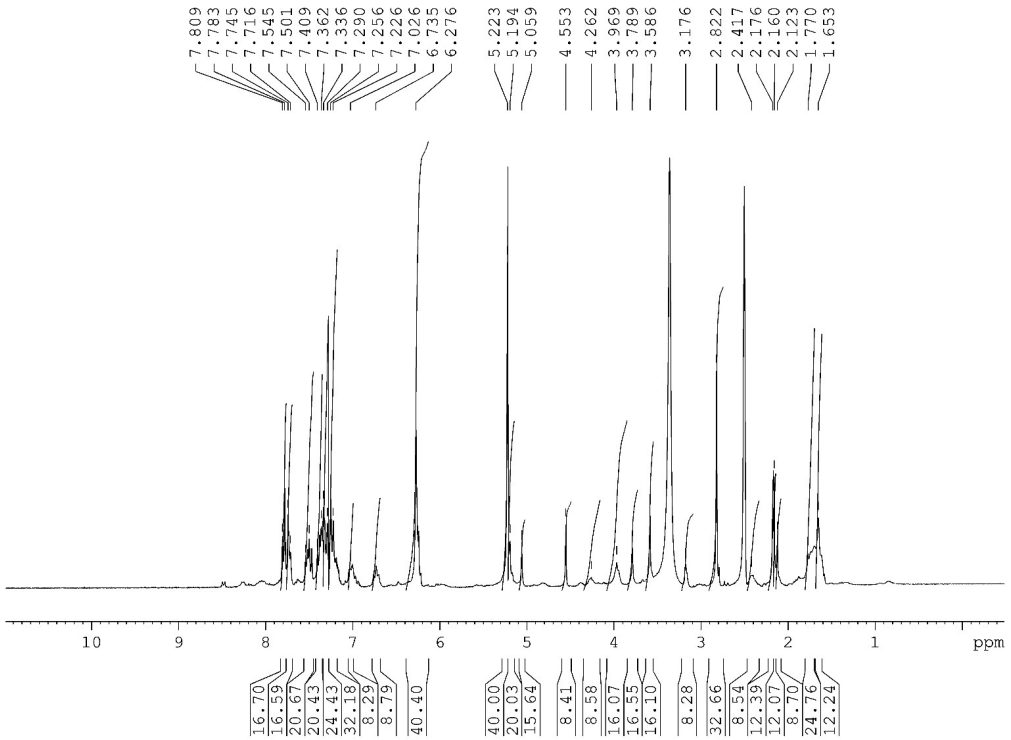

Figure 3. ^1H NMR spectra of **D5-G1-I** in DMSO-d_6

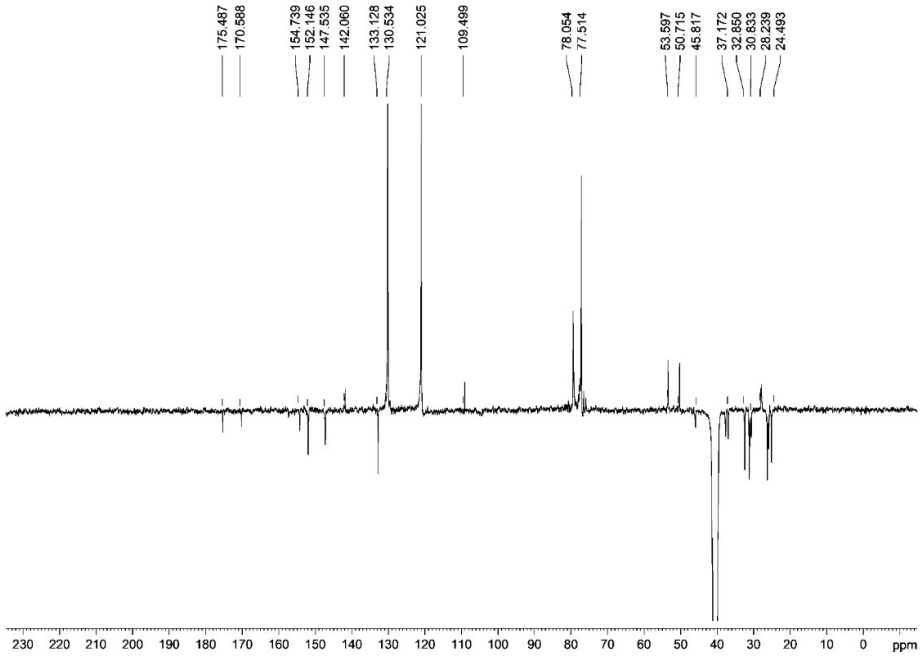

Figure 4. ^{13}C NMR spectra of **D5-G1-I** in DMSO-d_6

2.3.3 Sulindac-terminal dendrimer (D8-G3-S)

The preparation of D8-G3-S obeyed a process similar to the synthesis of D4-G1-S using a 1:12 ratio. Dendrimer D7-G2-OH (0.400 g, 0.023 mmol), sulindac (0.133 g, 0.371 mmol), DMAP (0.045 g, 0.371 mmol), DCC (0.076 g, 0.371 mmol), and 5 mL DMF were combined in a 25 mL round-bottom flask. The product's molecular weight is 22399 g/mol, yielding 77%. ATR-FTIR; ν_{max}/cm^{-1}: 2893 (Ar-C), 2856 (Cp-C), 1711 (CO), 1213 (C-O-C). ^1H NMR data d_H (300 MHz; DMSO-d_6): 7.78 (52H, s, uncompleted O-Ar-H), 7.74 (52H, s, uncompleted O-Ar-H), 7.50 (40H, s, sulindac SO-Ar-H + uncomplexed CO-Ar-H), 7.38-7.35 (96H, d, *J = 8.1 Hz*, uncomplexed Ar-H), 7.29 (32H, s, sulindac-Ar-H), 7.26-7.23 (32H, s, sulindac-Ar-H), 7.04-7.01 (16H, s, sulindac-Ar-H), 6.72 (8H, s, complexed Ar-H), 6.27 (104H, s, complexed Ar-H), 5.35 (16H, s, sulindac-aliph-H), 5.22 (120H, s, outer Cp-H), 5.11 (20H, s, inner Cp-H), 5.07 (48H, s, benzyl-CH_2), 4.55 (16H, s, Core- CH_2), 3.99 (8H, s, aliphatic-CH_2), 3.79 (8H, s, aliphatic-CH_2), 3.87 (32H, s, sulindac-CH_2), 3.18 (16H, s, aliphatic-CH_2), 2.82 (40H, s, aliphatic-CH_2 + Core), 2.38 (24H, s, complexed-CH_2), 2.16 (48H, s, sulindac-CH_3), 2.06 (24H, s, complexed-CH_2), 1.66 (84H, s, sulindac-CH_3). ^{13}C NMR d_c (75 MHz; DMSO-d_6): 175.83, 172.02, and 169.05 (C=O), 153.19, 150.59, 145.98, 131.55, and 103.14 (quat-C), 138.57, 128.68, 119.58, 119.35, 108.157, and 106.39 (complexed Ar-C), 77.39 (Cp-C), 78.79, 75.80, and 74.54 (complexed Ar-C), 58.95, 36.31, 31.16, 29.71, and 23.05 (CH_2), 51.99, 48.82, 26.60, and 17.56 (CH_3). The Elemental Analysis of $C_{1053}H_{936}O_{140}Fe_{28}P_{28}F_{184}S_{20}$, found %C: 57.05 and %H: 4.14, theoretically: %C: 56.74 and %H: 4.21.

2.3.4 Indomethacin-terminal dendrimer (D9-G2-I)

The second-generation dendrimer, D7-G2-OH, was used to couple indomethacin, in a process like the coupling of sulindac. In a 25 mL round-bottom flask, dendrimer D7-G2-OH (0.400 g, 0.023 mmol), sulindac (0.133 g, 0.371 mmol), DMAP (0.045 g, 0.371 mmol), DCC (0.076 g, 0.371 mmol), and 5 mL DMF were combined. The product's molecular weight is 22421 g/mol, yielding 77%. ATR-FTIR; ν_{max}/cm^{-1}: 2886 (Ar-C), 2826 (Cp-C), 1692 (CO), 1232 (C-O-C). ^1H NMR data d_H (300 MHz; DMSO-d_6): 7.68 (116H, d, *J = 8.7 Hz*, indomethacin-O-Ar-H + uncompleted O-Ar-H), 7.50 (52H, s, uncompleted O-Ar-H), 7.32-7.27 (136H, m, uncomplexed CO-Ar-H + indomethacin-Ar-H + uncomplexed Ar-H), 7.02 (16H, s, indomethacin-Ar-H), 6.25 (112H, s, complexed Ar-H), 5.21

(140H, s, Cp-H), 5.07 (48H, s, benzyl-CH_2), 4.55 (16H, s, CH_2), 3.88 (32H, s, indomethacin-CH_2 + aliphatic-CH_2), 3.76 (40H, s, core + indomethacin-CH_2), 3.66 (32H, s, aliphatic-CH_2), 2.37 (24H, s, complexed-CH_2), 2.22 (48H, s, indomethacin-CH_3), 2.07 (24H, s, complexed-CH_2), 1.67 (84H, s, indomethacin-CH_3 + complexed-CH_2). ^{13}C NMR dc (75 MHz; DMSO-d_6): 177.50 and 173.76 (CO), 152.72, 147.25, 141.77, and 135.23 (quat-C), 131.35, 130.08, 129.50, 121.13, 120.74, and 113.77, (uncomplexed Ar-C), 78.72 (Cp-C), 76.01 and 75.47 (complexed Ar-C), 63.13, 45.76, 31,27, and 27.77 (CH_2-C), 36.64, 31.63, and 30.67 (CH_3-C). The Elemental Analysis of $C_{1037}H_{920}O_{156}N_{16}Fe_{28}P_{28}F_{168}Cl_{16}S_4$, found: %C: 56.03, %N: 1.05, and %H: 4.19, theoretically: %C: 55.55, %N: 1.00, and %H: 4.14.

2.3.5 Sulindac-terminal dendrimer (D12-G3-S)

The synthesis of D12-G3-S followed a procedure similar to the one used for D4-G1-S and a ratio of 1:24 was used. A 25 mL round-bottom flask was charged with dendrimer D11-G3-OH (0.550 g, 0.021 mmol), sulindac (0.181 g, 0.508 mmol), DMAP (0.105 g, 0.508 mmol), DCC (0.062 g, 0.508 mmol), and 5 mL DMF.

The product's molecular weight is 46958 g/mol, yielding 82%. ATR-FTIR; ν_{max}/cm^{-1}: 2887 (Ar-C), 2864 (Cp-C), 1699 (CO), 1203 (C-O-C). ^{1}H NMR data d_H (300 MHz; DMSO-d_6): 7.77 (116H, s, uncompleted O-Ar-H), 7.73 (116H, s, uncompleted O-Ar-H), 7.50 (72H, m, sulindac SO-Ar-H + uncomplexed CO-Ar-H), 7.35 (224H, d, *J = 8.1 Hz*, uncomplexed Ar-H), 7.25 (96H, s, sulindac-Ar-H), 7.02 (64H, s, sulindac-Ar-H), 6.73 (8H, s, complexed Ar-H), 6.25 (224H, s, complexed Ar-H), 5.33 (32H, s, sulindac-aliph-H), 5.21 (300H, s, Cp-H), 5.10 (112H, s, benzyl-CH_2), 4.55 (16H, s, core-CH_2), 3.96 (16H, s, aliphatic-CH_2), 3.78 (60H, s, sulindac-CH_2 + aliphatic-CH_2), 2.81 (60H, s, sulindac-CH_2 + aliphatic-CH_2), 2.42 (56H, s, complexed-CH_2), 2.39 (96H, s, sulindac-CH_3), 2.15 (56H, s, complexed-CH_2), 1.66 (180H, s, sulindac-CH_3 + complexed-CH_3). ^{13}C NMR d_C (75 MHz; DMSO-d_6): 175.58, 172.61, and 170.72 (CO), 160.67, 158.21, 157.52, 155.94, 148.25, 147.66, 121.05, 109.71, and 100.74 (quat-C), 130.12, 118.48, 114.74, 114.15, 110.50, and 99.85 (uncomplexed Ar-C), 77.256 (Cp-C), 78.88 and 74.83 (complexed Ar-C), 64.56, 58.95, 53.60, 49.85, 44.56, 38.20, 27.09, and 17.56 (CH_2), 36.93, 29.71, and 14.18 (CH_3). The Elemental Analysis of $C_{2221}H_{1904}O_{284}Fe_{60}P_{60}F_{392}S_{36}$: calculated %C: 56.81 and %H: 4.10, found %C: 56.10 and %H: 4.05, found %C: 57.38 and %H: 4.11, theoretically: %C: 56.81 and %H: 4.10.

2.3.6 Indomethacin-terminal dendrimer (D13-G3-I)

In this experiment, the third-generation dendrimer, D11-G3-OH, was used to couple indomethacin in a process similar to the coupling of sulindac. The experiment was conducted using a 25 mL round-bottom flask containing D11-G2-OH dendrimer (0.550 g, 0.021 mmol), indomethacin (0.240 g, 0.508 mmol), DMAP (0.105 g, 0.508 mmol), DCC (0.062 g, 0.508 mmol), and 5 mL DMF.

The product's molecular weight is 46890 g/mol, yielding 83%. ATR-FTIR; ν_{max}/cm^{-1}: 2906 (Ar-C), 2852 (Cp-C), 1707 (CO), 1221 (C-O-C). ^{1}H NMR data d_H (300 MHz; DMSO-d_6): 7.64 (128H, s, indomethacin-Ar-H), 7.54 (116H, s, uncompleted O-Ar-H), 7.30 (188H, s, uncompleted O-Ar-H + indomethacin-Ar-H), 7.04 (224H, s, uncomplexed Ar-H), 6.93 (32H, s, indomethacin-Ar-H), 6.26 (232H, s, complexed Ar-H), 5.22 (412H, br s, Cp-H + benzyl-CH_2), 4.56 (16H, s, core-CH_2), 3.86 (136H, s, indomethacin-CH_2 + aliphatic-CH_2), 2.42 (56H, s, complexed-CH_2), 2.21 (96H, s, indomethacin-CH_3), 2.12 (56H, s, complexed-CH_2), 1.63 (180H, s, indomethacin-CH_3 + complexed-CH_3). ^{13}C NMR d_c (75 MHz; DMSO-d_6): 178.37, 176.35, and 174.33 (CO), 160.47, 158.24, 155.62, 148.14, 133.79, and 120.65 (quat-C), 131.77, 127.53, 126.52, 111.76, and 99.84 (uncomplexed Ar-C), 78.95 (Cp-C), 76.94 and 74.06 (complexed Ar-C), 58.00, 54.46, 45.82, 38.40, 29.39, 25.93, and 23.24 (CH_2-C), 37.19 and 14.75 (CH_3-C). The Elemental Analysis of $C_{2181}H_{1872}O_{316}N_{32}Fe_{60}P_{60}F_{360}Cl_{32}S_4$, %C: 55.66, %N: 0.93, and %H: 4.08, theoretically: %C: 55.87, %N: 0.96, and %H: 4.01.

2.4 Biological Measurements

2.4.1 Antibacterial Assay

To determine the minimum inhibitory concentration (MIC) of dendrimers, the broth microdilution technique was utilized.[54] The bacteria E. coli and M. luteus were grown in a nutrient broth at a temperature of 37°C. Dendrimers dissolved in dimethyl sulfoxide (DMSO) were applied to bacteria in their early log phase (with an optical density of approximately 0.1 at 600 nm) at varying concentrations ranging from 3.12 µM to 100 µM for 18 hours. Following the incubation, the bacterial culture medium was diluted at different ratios (ranging from 1 in 1000 to 1,000,000) in sterile PBS and then plated on agar. The plates were subsequently incubated at 37 °C for 24 hours to ascertain the MIC value.

2.4.2 Cell Cytotoxicity Assay

Monocyte/macrophage-like cells, known as RAW 264.7 cells, were cultured in DMEM/F12 supplemented with 10% FBS and 100 IU/ml penicillin and streptomycin at 37 °C in 5% CO_2. 1×10^6 cells/ml were seeded in a 96-well microplate. Cells in the growth phase, approximately 70% confluency, were treated with various concentrations (1 µM to 100 µM) of dendrimers for 24 hours. The cell viability was determined in triplicate using the CellTiter 96® Aqueous Cell Proliferation Assay, in accordance with the manufacturer's instructions. The half-maximal inhibitory concentration (IC_{50}) value was used to evaluate the cellular toxicity of the samples, and the percentage cell viability was calculated using a specific formula:

$$\%\ Cell\ Viability = \frac{absorbance\ of\ sample - absorbace\ of\ negative\ control}{absorbance\ of\ positive\ control - absorbace\ of\ negative\ control}\ X\ 100$$

The cells incubated with phosphate buffered saline (PBS) served as the positive control, while the negative control consisted of media.
Make it persuasive.

2.4.3 Cytokine Secretion Studies

The immunomodulatory effect of different drugs and dendrimers was evaluated on LPS-activated RAW 264.7 macrophage. These include indomethacin, a nonsteroidal anti-inflammatory drug, and sulindac, an antibacterial drug. Dendrimers without drugs and drug-conjugated dendrimers of different generations (G1-G3) were also included.
To conduct the study, cells at a density of 1×10^6 cells/ml in a 96-well microplate were seeded. The cells were treated with dendrimer samples diluted in serum-free DMEM/F12 medium at the final concentration of 2.6µM, in the presence of 1 µg/mL of lipopolysaccharide (LPS), and cytokine secretion was measured using relevant Enzyme-linked Immunosorbent Assay (ELISA) kits. The cells were also treated with 1 µg/mL LPS alone, as a control. The cell culture supernatant was collected after 24 hours, and ELISA was used to quantify the production of Interleukin 10 (IL-10), Tumor necrosis factor α (TNF-α), and interleukin-1β (IL-1β) in triplicate.

3. RESULTS AND DISCUSSION

3.1 Syntheses and characterization of the dendrimers

The new dendrimers were successfully synthesized, attached to indomethacin, and sulindac functionalized for the first to the third generation. These reactions resulted in a yield of between 60-80%, and protection steps were unnecessary. Schemes 1-4 depict the drug conjugation process with the dendrimers, which various techniques were used to characterize and identify. The zero-generation D1-G0-COOH, first D2-G1-Cl, and D3-G1-OH were synthesized in the previous study.[53] Then, the hydroxyl group in D3-G1-OH was used to attach the indomethacin and sulindac carboxylic group by ester linkage through the esterification reaction, as shown in Schemes 1 and 2, resulting in D4-G1-S and D5-G1-I.

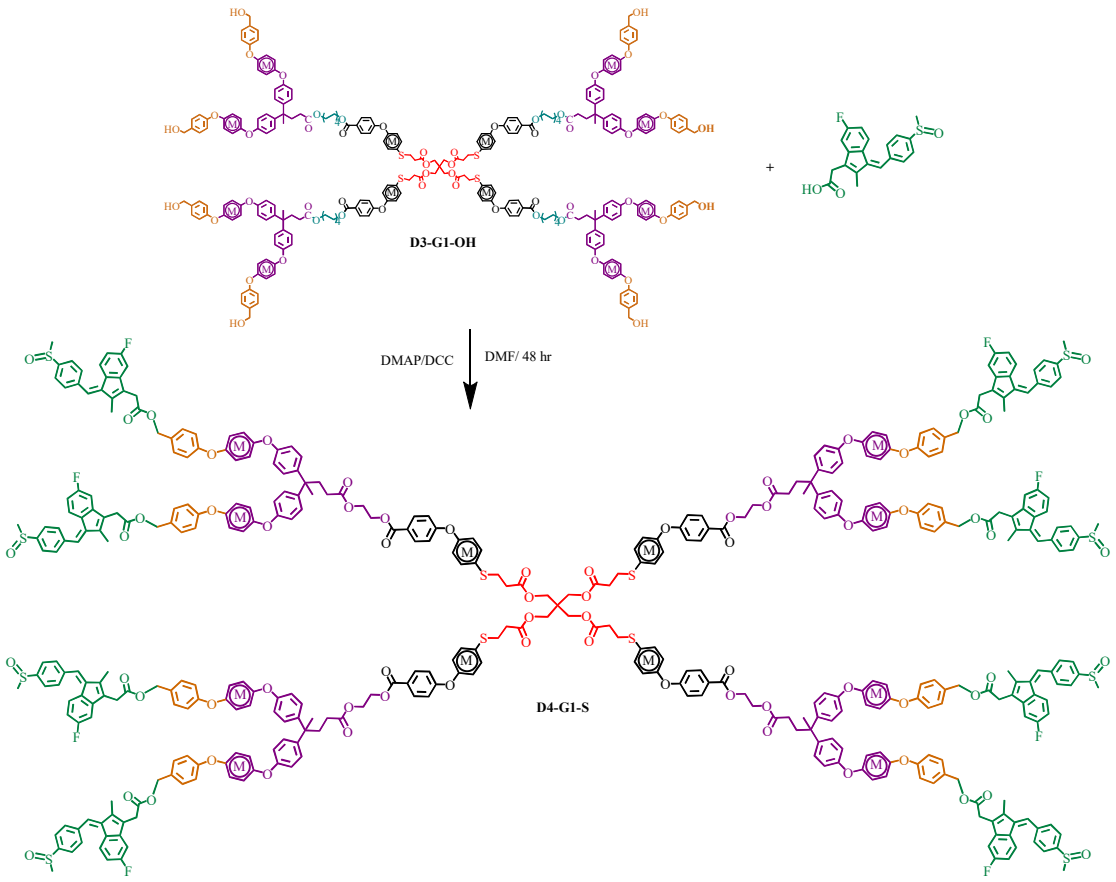

Scheme 1. Schematic representation of the synthesis of first-generation dendrimer 4 **(D4-G1-S)**.

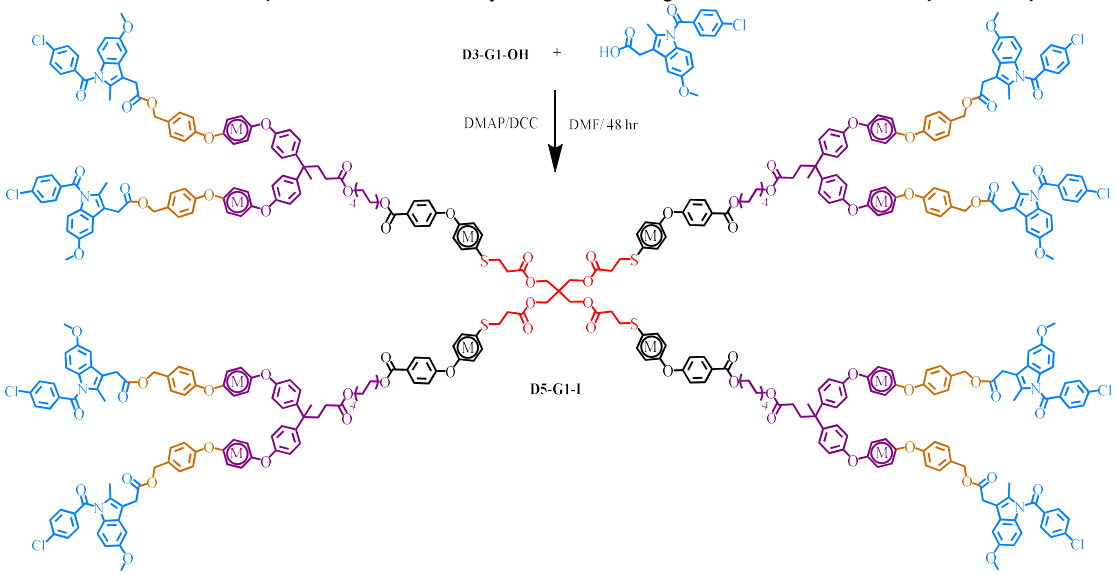

Scheme 2. Schematic representation of the synthesis of first-generation dendrimer 5 **(D5-G1-I)**.

The second D6-G2-Cl and D7-G2-OH were synthesized in the previous study.[53] Then the indomethacin and sulindac were attached to D7-G2-OH by esterification reaction to form D8-G2-S and D9-G2-I as illustrated in Scheme 3.

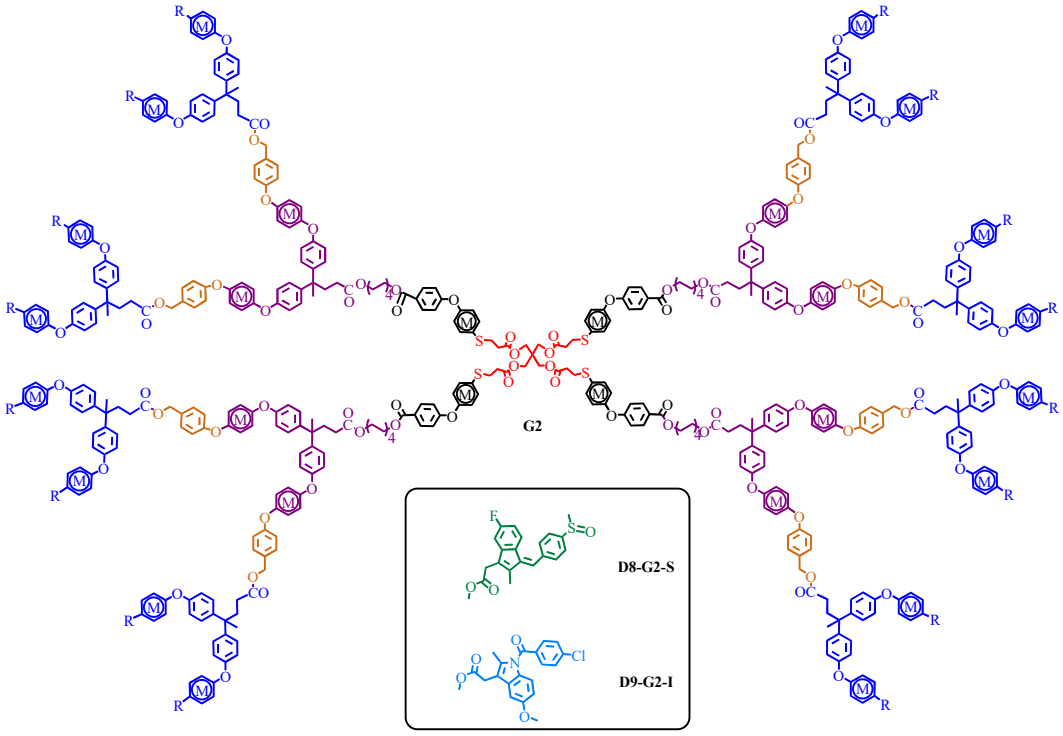

Scheme 3. The synthesis of the second-generation dendrimers **(D8-G2-S)** and **(D9-G2-I)**.

The previous study synthesized Third D10-G3-Cl and D11-G3-OH,[53] followed by the attachment of indomethacin and sulindac to D11-G2-OH through an esterification reaction, forming D12-G3-S and D13-G3-I as presented in Scheme 4.

The dendrimers synthesized in this project were characterized using ^{1}H and ^{13}C NMR spectroscopy, as well as IR. For instance, in the ^{1}H NMR spectrum of the zero-generation (D1-G0-COOH) dendrimer, a single peak at 6.49 ppm represented the 16 protons in the four complex outer aryl groups. Moving to the first-generation dendrimer (D2-G1-Cl), two peaks at 6.82 ppm and 6.44 ppm represented the protons in the complexed aryl groups. The downfield peak at 6.82 ppm referred to the outer complexed aryl groups attached to the peripheral chloro-end groups, while the upfield peak at 6.44 ppm referred to the inner complexed aryl groups attached to the etheric oxygen groups. After the chloro-end groups of D2-G1-cl were replaced by 4-hydroxylbenzyl alcohol to yield dendrimer D3-G1-OH, all the protons in the complexed aryl groups resonated upfield at 6.26 ppm as one peak due to the equivalent surrounding etheric oxygen groups.

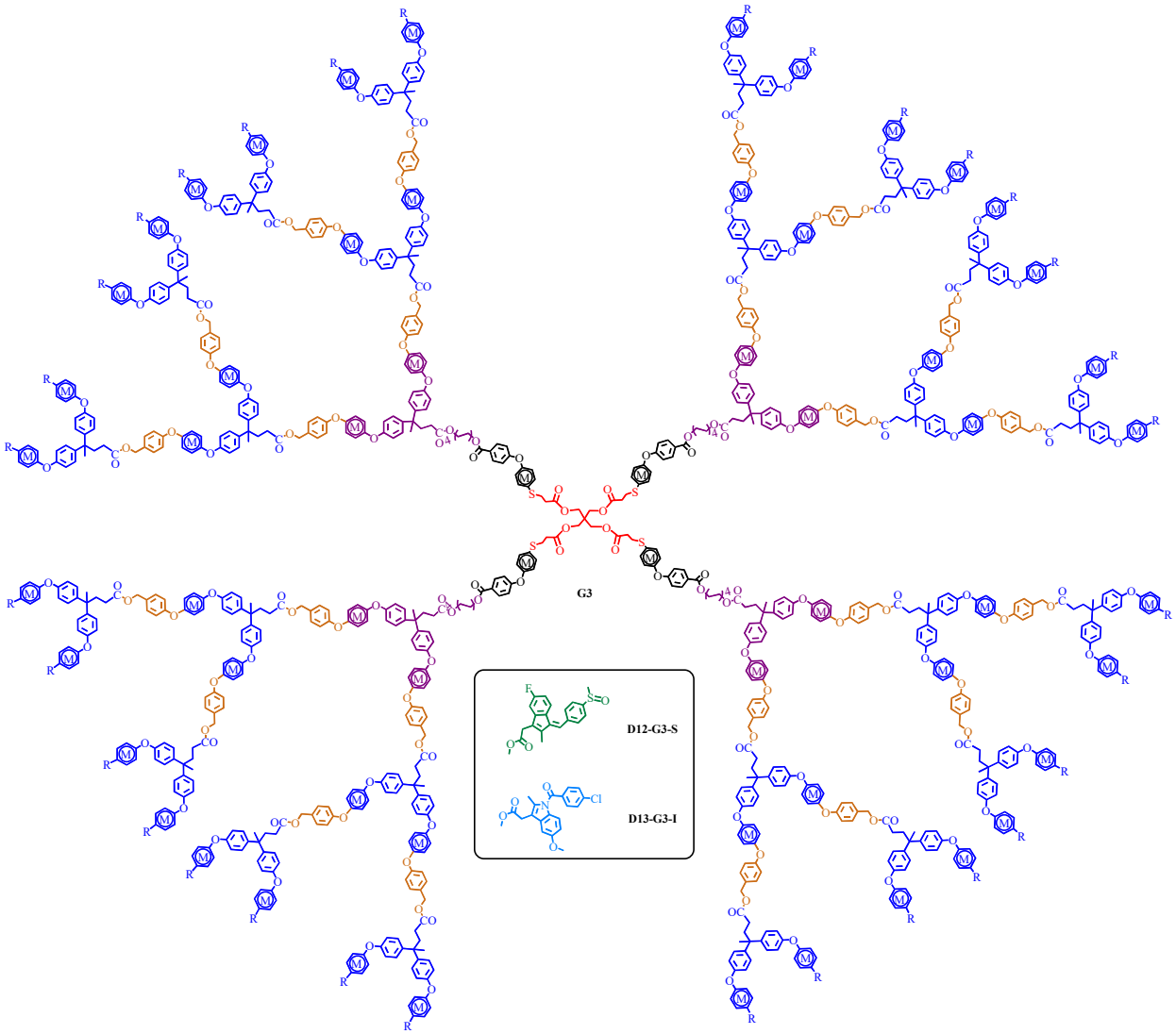

Scheme 4. The synthesis of the third-generation dendrimers **(D12-G3-S)** and **(D13-G3-I)**.

Additionally, in the second-generation dendrimer (D6-G2-Cl), the peak at 6.27 ppm represented all the protons of the inner complexed aryl groups, while the protons of the outer complexed aryl groups were represented by two peaks at 6.44 ppm and 6.81 ppm due to non-equivalent attached groups. As the generation of dendrimers increased, the peak broadened, and the peak intensities were consistently integrated based on the number of protons. In the zero-generation dendrimer (D1-G0-COOH), there was only one peak at 5.18 ppm standing for the protons of the Cp, but in the first-generation dendrimer (D2-G1-Cl), there were two peaks at 5.28 and 5.15 ppm representing the protons of the Cp. In the second-generation dendrimer (D6-G2-Cl), there were also two peaks representing the Cp with integration in agreement with the ratio of the protons of Cp in the periphery attached either to chloro-arenes or to the inner etheric oxygen groups.

^{13}C NMR spectroscopy was also used to confirm the structure of the dendrimers. For example, in the zero-generation dendrimer (D1-G0-COOH), there were two peaks for the carbonyl groups shown at 171.51 ppm and 167.35 ppm and one peak for the Cp carbons shown at around 80.11 ppm. In the first-generation dendrimer (D2-G1-Cl), two peaks were shown at around 80.23 ppm and 79.76 ppm for the

Cp carbons. Due to the presence of the chloro-end groups in the dendrimer D2-G1-Cl, the carbons of the complexed aryl groups resonated at around 87.69 ppm and 77.32 ppm, while the carbons of the complexed aryl groups with ether linkages resonated at around 76.05 ppm and 75.43 ppm. Uncomplexed carbons resonated around 130.00 ppm, and quaternary carbons were detected around 122.80 ppm. As the generation of the dendrimers increased, both ^{1}H and ^{13}C NMR spectra showed overlapped peaks.

For the new dendrimers, the first-generation dendrimer, D4-G1-S showed two peaks at 6.73 and 6.27 ppm, indicating the presence of 8 protons near the S-atom in the inner Cp groups and 40 equivalent protons in the twelve inner and outer complexed aryl groups attached to the etheric oxygen groups. Two additional peaks were observed at 5.22 and 5.19 ppm, corresponding to the protons in the outer and inner Cp groups, respectively. The successful incorporation of drug moieties with dendrimer D3-G1-OH was indicated by the absence of an OH peak in the NMR spectra. The composition of the synthesized dendrimers was confirmed through NMR and IR spectroscopy analyses. It was observed that the solubility of the dendrimers decreased in organic solvents as the molecular weight increased, although all dendrimers remained soluble in polar aprotic solvents like DMF and DMSO. Higher generations of dendrimers had broad and overlapping peaks. It was very difficult to distinguish between them, but the integrations and intensities of the peaks indicated the formation of the dendrimers.

3.2 Morphology Study

SEM was used to examine the surface structure of the dendrimers created. A comparison of the different generations, namely D5-G1-I, D9-G2-I, and D13-G3-I, is illustrated in Figure 5 with representative images. The samples were deposited on a metal surface coated with a 40-60 nm layer of gold and then observed under the microscope. As an example, the first generation (D5-G1-I) is shown in Figure 5-a. The sample appears to be amorphous with irregular shapes. Its structure lacks a defined or crystalline arrangement, resulting in a random and disordered appearance. The surface is marked by irregular contours and unpredictable boundaries, devoid of any recognizable pattern. This unique and diverse surface area enhances its ability to interact with its surroundings and makes it an interesting specimen to study. The rugged and textured surface of the second-generation (D9-G2-I) rock structure is marked by irregular bulky particle distribution, giving it a distinct appearance from the amorphous surface of the first generation (Figure 5-b). Moving on to the third-generation dendrimer (D13-G3-I), it exhibits a crystal-like morphology with sharp edges. Its structure has a distinct shape from the other generations, suggestive of a regular and ordered arrangement of atoms, resulting in a visually sharp and defined appearance (Figure 5-c).

Upon conducting SEM analysis, it was determined that there were slight differences in the surface morphology between dendrimer generations. Both the first and second generations exhibited irregular amorphous structures with rough and uneven surfaces, indicating that the transition from the first to the second generation did not significantly impact the surface morphology. However, the third generation displayed a distinct and more designed structure, suggesting that further advancements were made in the design and synthesis of dendrimers.

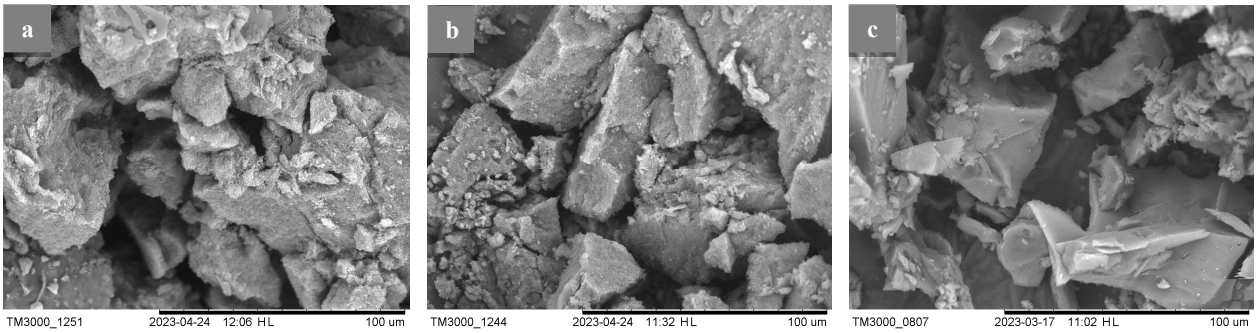

Figure 5. SEM images a) D5-G1-I**,** b) D9-G2-I, c) D13-G3-I.

3.3 Electrochemical Characteristics

The electrochemical behaviour of the synthesized dendrimers was studied using cyclic voltammetry (CV) at 0 ºC. The tests were carried out in a three-electrode cell setup comprising a Pt wire as the counter electrode, a glassy carbon electrode as the working electrode, and Ag/AgCl as the reference electrode. Cyclic voltammetry involves cycling the potential back and forth between two values to investigate the redox behaviour of the species in solution. In this instance, the potential was cycled from 0.0 to -2.0 V at a scan rate of 100 mV/s. The scan rate indicates the speed at which the potential changes per unit of time. To facilitate the electrochemical measurements, a supporting electrolyte (Bu4NPF6) was used. The supporting electrolyte helps to improve the conductivity of the solution and provides a medium for the movement of ions. The synthesized dendrimers displayed reversible behavior in cyclic voltammetry, which was attributed to the existence of redox-active iron centers within their dendritic branches. These iron centers (η^6-aryl-η^5-cyclopentadienyliron(II)) are responsible for the efficient electron transfer processes and readily reversible redox reactions.

The number of redox centers increased with each dendritic generation. However, there were no significant changes in the reduction and oxidation values, as shown in Figure 6. This indicates that the electrochemical properties of the dendrimers remain consistent as the dendritic generation increases. Across all generations (G1 to G3), the dendrimers exhibited reversible reduction with an average half-wave potential (E1/2) value of approximately -1.25 V.[25] The intensity of the reduction and oxidation peaks grew as the dendritic generation increased from G1 to G3. This is likely due to the more significant number of iron centers in the higher generations than G1.[55] The absence of peak splitting in the higher generations (G2 and G3) is consistent with previous reports, indicating the electron transfer rate between the electrodes and iron centers becomes faster.[55,56] The high-speed electron transfer prevents the splitting of the redox wave into separate peaks. Furthermore, the dendritic arms are flexible, ensuring that all iron centers experience a close enough environment to lead to a single redox peak.

The consistent electrochemical properties and reversible behavior of the dendrimers with increasing generation suggest their potential utility in various applications such as electrocatalysis, energy storage, or sensing.

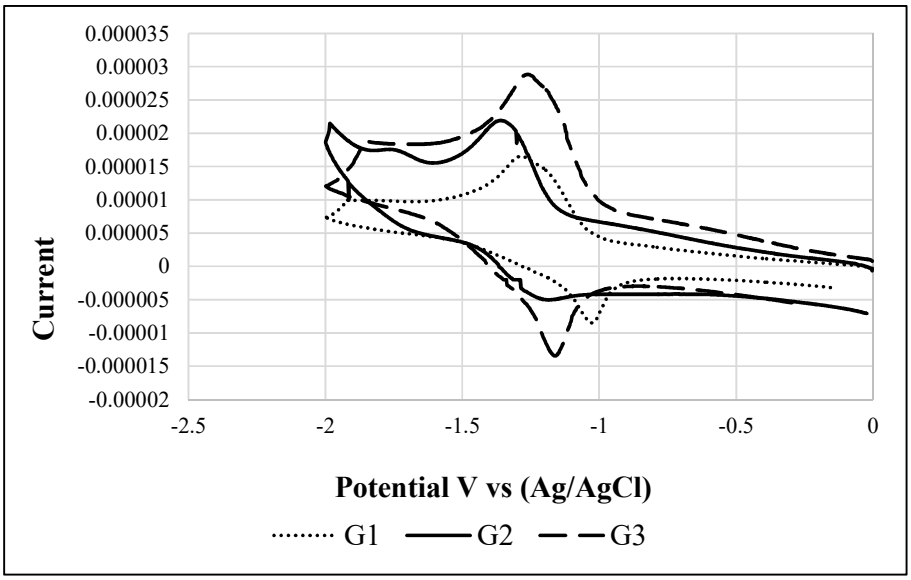

Figure 6. Cyclic voltammogram representative, at a scan rate of 2.0 V/s, was obtained in propylene carbonate with 0.1 M Bu_4NPF_6 at a temperature of 0°C. …….. **(**D4-G1-S**),** —— **(**D8-G2-S**),** ------- **(**D12-G3-S**).**

3.4 Thermogravimetric Analysis

The TGA was employed to analyze how the dendrimers degrade and decompose when subjected to increasing temperatures from 0 to 1000°C. TGA involves subjecting the dendrimers to a constant heating rate in a nitrogen atmosphere and the weight loss indicates the degradation and decomposition of the dendrimers at different stages as a function of temperature. According to the TGA results, the dendrimers showed thermal stability up to 200°C, indicating that they did not undergo significant decomposition up to this temperature (see Figure 7). However, above 200°C, the thermal decomposition process started, leading to a mass loss of approximately 18-30%. This suggests that the decomposition process at the specific temperature of 200°C involves the degradation or removal of the cationic cyclopentadienyl iron component within the dendrimers.[34,57] At a temperature of 200°C, G1 experienced a weight reduction of about 30%. In contrast, the subsequent G2 only had a weight loss of roughly 18%, while G3 displayed a weight reduction of approximately 22%. As the temperature rose, the degradation process sped up, causing a significant decrease in weight between 300°C and 400°C. The dendrimers lost about 60% of their weight within this temperature range. Specifically, G1 underwent a second substantial weight loss at 400°C, and its decomposition continued until nearly 650°C. G2 exhibited the second stage of degradation earlier than G1, occurring between 300°C and 600°C and resulting in a weight loss of about 65%. G3 also displayed a second stage of degradation with a weight loss of approximately 55% between 400°C and 600°C. After the second stage of degradation, all dendrimers showed a final weight reduction of about 20% when heated to 900 °C. Residual contents containing iron oxide and phosphorus oxide residues were found after the TGA analysis.[25] The overall TGA results suggested that the dendrimers exhibited a collective mass reduction of around 80% within the temperature range of 200-900°C, indicating their thermal stability.

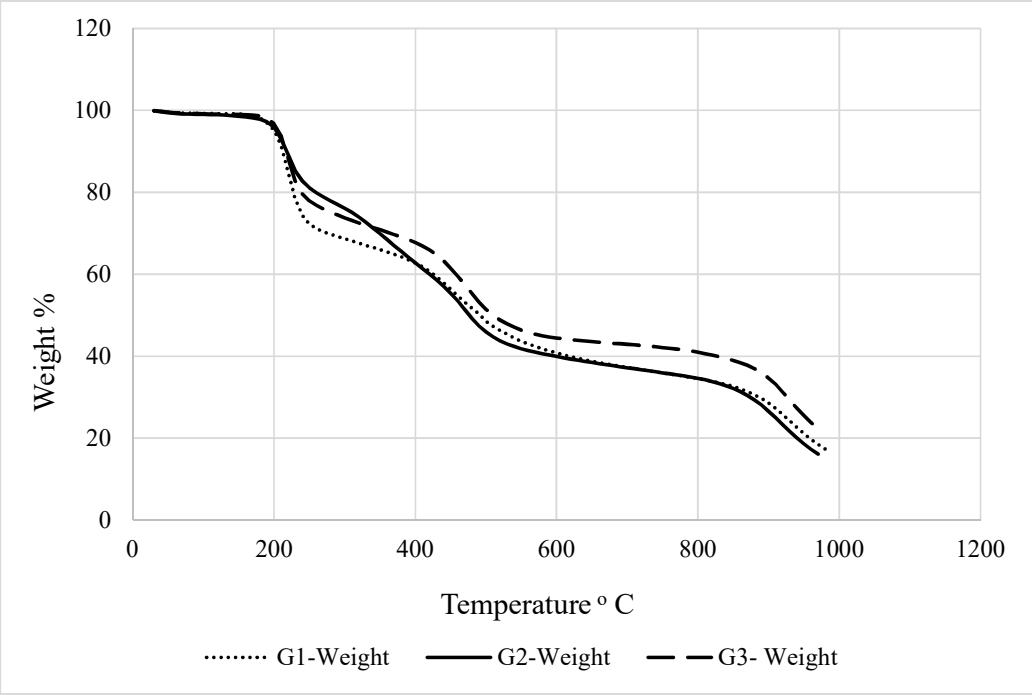

Figure 7. TGA representative of the three generations, …….. (D4-G1-S), _____ (D8-G2-S), ------- (D12-G3-S).

3.5 Bacterial and Cellular Toxicity

To combat the antibacterial efficacies of metallodendrimers with and without attached drugs were first tested against gram-negative (*E.coli*) and gram-positive (*M.luteus*) bacterial strains.[58-61] Our results indicated that most of the synthesized dendrimers were ineffective against the two types of bacteria.[62-64]

Table 1 displays the (MIC) value of the dendrimers, which indicates some antibacterial activity. According to prior research, samples exhibit antibacterial activity when they are soluble or dispersed below their critical micelle concentration (CMC) values. However, samples from the micelles that are above the CMC values are unable to exhibit any antimicrobial features.[65,66]

The dendrimers attached to indomethacin and sulindac did not significantly impact the antibacterial activity of the dendrimers at all studied concentrations (below and above CMC). Among the various dendrimers tested, it was found that D7-G2-OH showed some antibacterial activity, albeit at high concentrations (50µM) against both *M.luteus* and *E.coli,* while D5-G1-I displayed antibacterial activity at 50 µM concentration against *E.coli* only. Overall, drug-loaded dendrimers lack generation-dependent antibacterial activity and only some bacterial killing at high concentrations of certain dendrimers is observed.

The cytotoxicity of dendrimers and their drug conjugates was then tested on RAW 264.7 cell line, by MTS assays. Interestingly, the dendrimers alone and their drug conjugates showed generation-dependent toxicity in macrophages and toxicity of dendrimers was decreased as a function of generation of dendrimers. The first-generation dendrimers and their conjugates were more toxic than the higher-generation ones, possibly due to the better solubility and stability of lower-generation dendrimers under physiological conditions. The attachment of hydrophobic drugs to the hydrophilic functional groups of dendrimers overall reduced the cytotoxicity of the dendrimers, possibly due to reduced solubility and physiological availability of the conjugates. This was further supported by the fact that IC_{50} values of dendrimers alone were lower than their CMC values, indicating the role of individual dendrimer molecules in cellular interactions. The drug-conjugated dendrimers, on the other hand, showed IC_{50} values at or above CMCs indicating that self-assembly of dendrimers in the form of aggregates

dictates their biological properties. The IC_{50} values, antibacterial efficacies and CMCs of dendrimers and their conjugates are outlined in detail in Table 1.

Table 1. MIC and IC_{50} value of Dendrimers

Metallodendrimers	MIC (µM)		IC_{50} (µM)	CMC (µM)
	E.coli	*M.Luteus*		
D4-G1-S	100<	100<	12.5	15.62
D5-G1-I	50	100	12.5	7.8
D8-G2-S	100<	100<	50	15.62
D9-G2-I	100	100<	50	3.9
D12-G3-S	100	100<	100	7.8
D13-G3-I	100	100<	100	7.8
D3-G1-OH	100<	100	3.12	3.9
D7-G2-OH	50	50	3.12	15.62
D11-G3-OH	100	100<	6.25	15.62

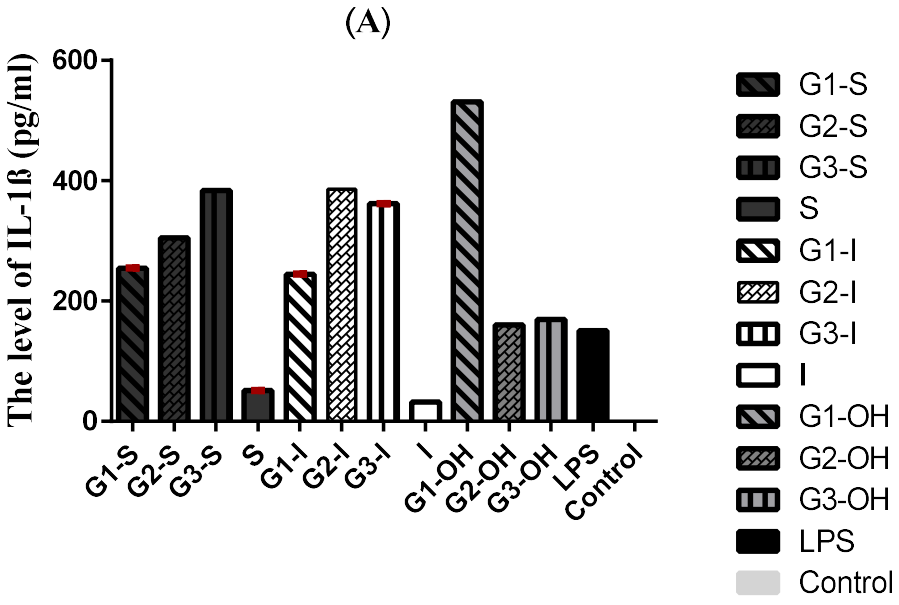

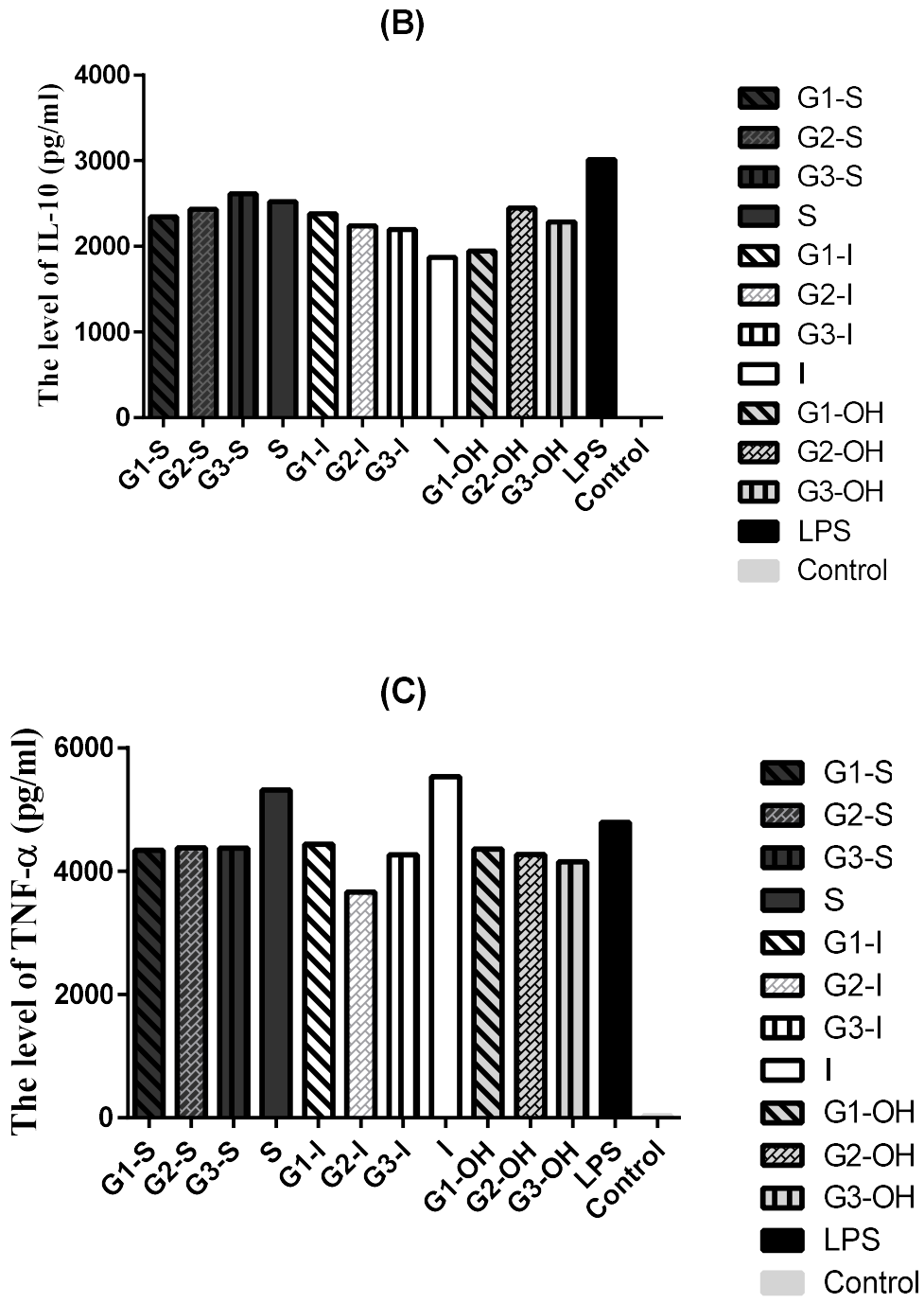

Figure 8. Cytokine release (**A**) IL-10, (**B**), ad IL-1β and (**C**) TNF-α was performed by ELISA from Raw 264.7 cell line upon treatment with LPS, peptides and drugs. Error bars indicate the standard deviation of three replicates. The macrophage was treated with the dendrimers upon LPS challenge and data was expressed as the mean ± SD (n=3) p (p-value < 0.0001).
Abbreviation: S: Sulindac, I: Indomethacin, G1-S: D4-G1-S, G2-S: D8-G2-S, G3-S: D12-G3-S, G1-I: D5-G1-I, G2-I: D9-G2-I, G3-I: D13-G3-I.

3.6 Cytokine Release Study

The human body responds to infections, toxins, and injuries through a complex process called inflammation. This process involves macrophages releasing inflammatory mediators like IL-1β, IL-10, and TNF-α.[67-69] However, excessive and prolonged activation of macrophages can lead to acute or chronic inflammatory conditions like chronic hepatitis, atherosclerosis, and rheumatoid arthritis.[70-72] Inhibition or reduction of pro-inflammatory cytokine production might be a suitable therapeutic strategy in inflammatory diseases.[73]

In this study, the anti-inflammatory properties of dendrimers alone and their drug-conjugated analogues were investigated *in vitro*. The macrophages were exposed to dendrimers and their drug conjugates at a concentration lower than IC50 (2.6 μM) while in the presence of 1 μg/mL of LPS. The ELISA assay was used to assess the production of cytokines (IL-1β, IL-10, and TNF-α).[74-77] As shown in Figure 8, sulindac and indomethacin remarkably inhibit the secretion of IL-1β in LPS-stimulated RAW264.7 macrophages, validating their potential as NSAIDs. The conjugation of drugs with dendrimers abrogated LPS neutralizing and anti-inflammatory capabilities of NSAIDs and IL-1β production was not inhibited by the dendrimers alone or their drug conjugates. In fact, first-generation drug-free dendrimer promoted pro-inflammation, compared to controls, while the inflammation capabilities of higher-generation dendrimers and all drug conjugates were lower possibly due to lower solubility and stability of these macromolecules.

TNF-α and IL-10 pro-inflammatory and anti-inflammatory cytokines that are not directly related to inflammasome activation were also tested and as shown in Figures 8B & C. Interestingly, NSAID showed a slight reduction in IL-10 production and over-expression of TNF-α production, however, all the dendrimers and their drug conjugates showed only marginal effect on pro and anti-inflammatory cytokine production, post-LPS treatment, compared to LPS alone treatment.

Our results demonstrate that first-generation dendrimers alone can activate IL-1β production, possibly by the activation of inflammasome. The NSAID-dendrimers conjugates, however, do not show significant anti-inflammatory effects in vitro in LPS-induced inflammation in Raw 264.7 cells.

CONCLUSION

A new series of dendrimers, comprising 60 iron complexes and biologically active molecules, has been successfully created. The synthesis process involved integrating sulindac and indomethacin into the outer layer of the dendrimer. Various methods, including ^{1}H &^{13}C NMR and IR, were used to comprehensively analyze the structures of the dendrimers. The surface characteristics of the dendrimers from all generations were examined using SEM, revealing some morphological variations among the different generations. Additionally, TGA was utilized to explore the high thermal stability of the dendrimers. Furthermore, electrochemical experiments were carried out to investigate the redox behaviours of all dendrimers at different generations, demonstrating a single reversible redox wave with varying intensities based on the generation of the dendrimer. Through biological analysis, it has been demonstrated that unconjugated dendrimers possess overall antibacterial behavior and can induce pro-inflammation as a function of dendrimer generation. However, conjugating dendrimers with NSAIDs compromises their antibacterial efficacies and the anti-inflammatory effects of drugs are reduced due to on large sizes, and poor solubility of the conjugates that compromise the interactions between macromolecules and biological membranes. To ensure safety, toxicity tests were conducted on mammalian cell lines, which revealed that dendrimers connected to drugs were less toxic compared to others. Notably, the best-performing dendrimers were D7-G2-OH and D5-G1-I. According to these findings, the combination of sulindac and indomethacin with dendrimers can greatly enhance the effectiveness of drugs in reducing inflammation by preventing the secretion of TNF-α in Raw 264.7 cells. Future research will delve into the effects of different NSAIDs on the antibacterial and anti-inflammatory activities of their dendrimer conjugates. The current findings reveal the potential of dendrimers as promising therapeutic agents, and their ability to be conjugated with drugs further enhances their efficacy and specificity.

CONFLICT OF INTEREST

The authors declare no conflict of interest.

REFERENCES:

1. Soares, S.; Sousa, J.; Pais, A.; Vitorino, C. *Front. Chem.* **2018**, *6*, 360.
2. Tinkle, S.; McNeil, S.E.; Mühlebach, S.; Bawa, R.; Borchard, G.; Barenholz, Y.; Tamarkin, L.; Desai, N. *Ann. N. Y. Acad. Sci.* **2014**, *1313*, 35-56.
3. Nikzamir, M.; Hanifehpour, Y.; Akbarzadeh, A.; Panahi, Y. A Review. *J. Inorg. Organomet. Polym. Mater.* **2021**, *31*, 2246-2261.
4. Mekuria, S.L.; Li, J.; Song, C.; Gao, Y.; Ouyang, Z.; Shen, M.; Shi, X. *ACS Appl. Bio Mater.* **2021**, *4*, 7168-7175.
5. Tang, Y.; Ya-Ting Huang, A.; Chen, P.; Chen, H.; Kao, C. *Curr. Pharm. Des.* **2011**, *17*, 2308-2330.
6. Mhlwatika, Z.; Aderibigbe, B.A. *Molecules* **2018**, *23*, 2205.
7. D'Emanuele, A.; Attwood, D. *Adv. Drug Deliv. Rev.* **2005**, *57*, 2147-2162.
8. Zhang, C.; Pan, D.; Li, J.; Hu, J.; Bains, A.; Guys, N.; Zhu, H.; Li, X.; Luo, K.; Gong, Q. *Acta Biomater.* **2017**, *55*, 153-162.
9. Morgan, M.T.; Nakanishi, Y.; Kroll, D.J.; Griset, A.P.; Carnahan, M.A.; Wathier, M.; Oberlies, N.H.; Manikumar, G.; Wani, M.C.; Grinstaff, M.W. *Cancer Res.* **2006**, *66*, 11913-11921.
10. Taratula, O.; Schumann, C.; Duong, T.; Taylor, K.L.; Taratula, O. *Nanoscale* **2015**, *7*, 3888-3902.
11. Kobayashi, H.; Jo, S.; Kawamoto, S.; Yasuda, H.; Hu, X.; Knopp, M.V.; Brechbiel, M.W.; Choyke, P.L.; Star, R.A. *J. Magn. Reson. Imaging.* **2004**, *20*, 512-518.
12. Klajnert, B.; Cortijo-Arellano, M.; Bryszewska, M.; Cladera, J. *Biochem. Biophys. Res. Commun.* **2006**, *339*, 577-582.
13. Tarach, P.; Janaszewska, A. *Int. J. Mol. Sci.* **2021**, *22*, 2912.
14. Madaan, K.; Kumar, S.; Poonia, N.; Lather, V.; Pandita, D. *J Pharm Bioallied Sci.* **2014**, *6*, 139.
15. Rabiee, N.; Ahmadvand, S.; Ahmadi, S.; Fatahi, Y.; Dinarvand, R.; Bagherzadeh, M.; Rabiee, M.; Tahriri, M.; Tayebi, L.; Hamblin, M.R. *J. Drug Deliv. Sci. Technol.* **2020**, 101879.
16. Sherje, A.P.; Jadhav, M.; Dravyakar, B.R.; Kadam, D. *Int. J. Pharm.* **2018**, *548*, 707-720.
17. Liu, M.; Fréchet, J.M. *Pharm. Sci. Technol.* **1999**, *2*, 393-401.
18. Murugan, E.; Jebaranjitham, J.N. *Chem. Eng. J.* **2015**, *259*, 266-276.
19. Wiener, E.; Brechbiel, M.W.; Brothers, H.; Magin, R.L.; Gansow, O.A.; Tomalia, D.A.; Lauterbur, P.C. *Magn Reson Med Sci.* **1994**, *31*, 1-8.
20. Pan, B.; Cui, D.; Sheng, Y.; Ozkan, C.; Gao, F.; He, R.; Li, Q.; Xu, P.; Huang, T. *Cancer Res.* **2007**, *67*, 8156-8163.
21. Juris, A. *Annu. Rep. Prog. Chem. Sect. C: Phys. Chem.* **2003**, *99*, 177-241.
22. Xu, B.; Zhang, J.; Fang, H.; Ma, S.; Chen, Q.; Sun, H.; Im, C.; Tian, W. *Poly. Chem.* **2014**, *5*, 479-488.
23. Drobizhev, M.; Karotki, A.; Rebane, A.; Spangler, C.W. *Opt. Lett.* **2001**, *26*, 1081-1083.
24. Ghaddar, T.H.; Wishart, J.F.; Thompson, D.W.; Whitesell, J.K.; Fox, M.A. *J. Am. Chem. Soc.* **2002**, *124*, 8285-8289.
25. Abd-El-Aziz, A.S.; Benaaisha, M.R.; Abdelbaky, M.S.; Martinez-Blanco, D.; García-Granda, S.; Abdelghani, A.A.; Abdel-Rahman, L.H.; Bissessur, R. *Molecules* **2021**, *26*, 6732.
26. Balzani, V.; Ceroni, P.; Gestermann, S.; Kauffmann, C.; Gorka, M.; Vögtle, F. *Chem. Comm.* **2000**, 853-854.
27. Astruc, D.; Chardac, F. *Chem. Rev.* **2001**, *101*, 2991-3024.
28. Balzani, V.; Bergamini, G.; Ceroni, P.; Marchi, E. *New J. Chem.* **2011**, *35*, 1944-1954.
29. Yim, D.; Sung, J.; Kim, S.; Oh, J.; Yoon, H.; Sung, Y.M.; Kim, D.; Jang, W. *J. Am. Chem. Soc.* **2016**, *139*, 993-1002.

30. Grabchev, I.; Vasileva-Tonkova, E.; Staneva, D.; Bosch, P.; Kukeva, R.; Stoyanova, R. *New J. Chem.* **2018***, 42*, 7853-7862.
31. Wang, Y.; Salmon, L.; Ruiz, J.; Astruc, D. Nat. Commun. **2014***, 5*, 3489.
32. Hwang, S.; Shreiner, C.D.; Moorefield, C.N.; Newkome, G.R. *New J. Chem.* **2007***, 31*, 1192-1217.
33. Grabchev, I.; Staneva, D.; Vasileva-Tonkova, E.; Alexandrova, R.; Cangiotti, M.; Fattori, A.; Ottaviani, M.F. *J. Polym. Rese.* **2017***, 24*, 210.
34. Abd-El-Aziz, A.S.; Abdelghani, A.A.; El-Ghezlani, E.G.; Abou El-ezz, D.; Abdel-Rahman, L.H. *Macromol. Biosci.* **2020**, 2000242.
35. Abd-El-Aziz, A.S.; Benaaisha, M.R.; Abdelghani, A.A.; Bissessur, R.; Abdel-Rahman, L.H.; Fayez, A.M.; El-ezz, D.A. *Biomolecules* **2021***, 11*, 1568.
36. Zhang, Z.; Chen, F.; Shang, L. *Cancer. Manag. Res.* **2018***, 10*, 4631-4640.
37. Bindu, S.; Mazumder, S.; *Biochem. Pharmacol.* **2020***, 180*, 114147.
38. Andrews, J.; Djakiew, D.; Krygier, S.; Andrews, P. *Cancer Chemother. Pharmacol.* **2002***, 50*, 277-284.
39. Chan, E.W.L.; Yee, Z.Y.; Raja, I.; Yap, J.K.Y. *J. Glob. Antimicrob. Resist.* **2017***, 10*, 70-74.
40. Gauthier, M.J.; Rasouli, R.; Abd-El-Aziz, A.S.; Ahmed, M.; Abdelghani, A.A. *J. Inorg. Organomet. Polym. Mater.* **2023**, 33:3651–3664
41. Tinsley, H.N.; Mathew, B.; Chen, X.; Maxuitenko, Y.Y.; Li, N.; Lowe, W.M.; Whitt, J.D.; Zhang, W.; Gary, B.D.; Keeton, A.B. *Cancers* **2023***, 15*, 646.
42. Moore, R.A.; Derry, S.; McQuay, H.J. *Cochrane Database of Systematic Reviews* **2009**, Issue 4. Art. No.: CD007552.
43. Helleberg, L. *Clin. Pharmacokinet.* **1981***, 6*, 245-258.
44. Attiga, F.A.; Fernandez, P.M.; Weeraratna, A.T.; Manyak, M.J.; Patierno, S.R. *Cancer Res.* **2000***, 60*, 4629-4637.
45. Ricciotti, E.; FitzGerald, G.A. *Arterioscler. Thromb. Vasc. Biol.* **2011***, 31*, 986-1000.
46. [46] Di Costanzo, F.; Di Dato, V.; Ianora, A.; Romano, G. *Mar. Drugs.* **2019***, 17*, 428.
47. Kauppila, A.; Puolakka, J.; Ylikorkala, O. *Prostaglandins* **1979***, 18*, 647-653.
48. Brogden, R.N.; Heel, R.C.; Speight, T.M.; Avery, G.S. Sulindac: *Drugs* **1978***, 16*, 97-114.
49. Boardman, P.L.; Hart, F.D. *Ann. Rheum. Dis.* **1967***, 26*, 127.
50. Miliński, M.; Staś, M.; Beberok, A.; Wrześniok, D. *Pharmacol. Rep.* **2023**, 1-10.
51. Wiegand, I.; Hilpert, K.; Hancock, R.E. *Nat. Protoc.* **2008***, 3*, 163-175.
52. Neises, B.; Steglich, W. *Angew. Chem., Int. Ed. Engl.* **1978***, 17*, 522-524.
53. Abd-El-Aziz, A.S.; Abdelghani, A.A.; Wagner, B.D.; Abdelrehim, E.M. *Polym. Chem.* **2016***, 7*, 3277-3299.
54. Abd-El-Aziz, A.S.; May, L.J.; Hurd, J.A.; Okasha, R.M. *J. Polym. Sci., Part A: Polym. Chem.* **2001***, 39*, 2716-2722.Abd-El-Aziz, A.S.; Abdelghani, A.A.; Wagner, B.D.; Abdelrehim, E.M. *Polym. Chem.* **2016***, 7*, 3277-3299.
55. Abd-El-Aziz, A.S.; Abdelghani, A.A.; Wagner, B.D.; Pearson, J.K.; Awad, M.K. *Polymer* **2016***, 98*, 210-228.
56. Abd-El-Aziz, A.S.; Abdelghani, A.A.; Pearson, J.K.; Awad, M.K.; Overy, D.P.; Kerr, R.G. *Macromol. Chem. Phys* **2016***, 217*, 987-996.
57. Atatreh, N.; Youssef, A.M.; Ghattas, M.A.; Al Sorkhy, M.; Alrawashdeh, S.; Al-Harbi, K.B.; El-Ashmawy, I.M.; Almundarij, T.I.; Abdelghani, A.A.; Abd-El-Aziz, A.S. *Bioorg. Chem.* **2019***, 86*, 393-400.
58. Wise Jr, E.M.; Abou-Donia, M.M. *Proc. Natl. Acad. Sci.* **1975***, 72*, 2621-2625.
59. Sundström, L.; Rådström, P.; Swedberg, G.; Sköld, O. *Mol. Genet. Genom.* **1988***, 213*, 191-201.
60. Swedberg, G.; Sköld, O. *J. Bacteriol.* **1980***, 142*, 1-7.

61. Swedberg, G.; Fermér, C.; Sköld, O. *Chemistry and Biology of Pteridines and Folates* **1993**, 555-558.
62. Yin, Z.; Wang, Y.; Whittell, L.R.; Jergic, S.; Liu, M.; Harry, E.; Dixon, N.E.; Kelso, M.J.; Beck, J.L.; Oakley, A.J. *Chem. Biol.* **2014**, *21*, 481-487.
63. Zhang, Y.; Wu, J.; Zhou, H.; Huang, W.; Jia, B. *Infect. Microbes Dis.* **2020**, *2*, 77-82.
64. Eman, F.A.; Rehab, M.A.E.; Abo, B.F.A.; Nancy, G.F.; Neveen, A.A.; Gamal, F.M.G. *Afr. J. Microbiol. Res.* **2016**, *10*, 1408-1416.
65. Kurup, T.; Wan, L.; Chan, L.W. Preservative Requirements in Emulsions. **1992**.
66. Laatiris, A.; El Achouri, M.; Infante, M.R.; Bensouda, Y. *Microbiol. Res.* **2008**, *163*, 645-650.
67. Gery, I.; Gershon, R.K.; Waksman, B.H. *J. Exp. Med.* **1972**, *136*, 128-142.
68. Lyke, K.E.; Burges, R.; Cissoko, Y.; Sangare, L.; Dao, M.; Diarra, I.; Kone, A.; Harley, R.; Plowe, C.V.; Doumbo, O.K. *Infect. Immun.* **2004**, *72*, 5630-5637.
69. Wong, C.K.; Ho, C.Y.; Ko, F.; Chan, C.; Ho, A.; Hui, D.; Lam, C. *Clin. Exp. Immunol.* **2001**, *125*, 177-183.
70. Rooney, M.; David, J.; Symons, J.; Giovine, F.d.; Varsani, H.; Woo, P. *Rheumatology* **1995**, *34*, 454-460.
71. Riordan, S.M.; Skinner, N.A.; Kurtovic, J.; Locarnini, S.; McIver, C.J.; Williams, R.; Visvanathan, K. *J. Inflamm. Res.* **2006**, *55*, 279-285.
72. Autieri, M.V. *int. sch. res. notices.* **2012**, *2012*.
73. Szliszka, E.; Skaba, D.; Czuba, Z.P.; Krol, W. *Molecules* **2011**, *16*, 3701-3712.
74. Yoon, S.; Lee, Y.; Park, S.K.; Kim, H.; Bae, H.; Kim, H.M.; Ko, S.; Choi, H.Y.; Oh, M.S.; Park, W. *J. Ethnopharmacol.* **2009**, *125*, 286-290.
75. Kellum, J.A.; Song, M.; Li, J. *Am. J. Physiol. Regul. Integr. Comp. Physiol.* **2004**, *286*, R686-R692.
76. Khan, S.; Shin, E.M.; Choi, R.J.; Jung, Y.H.; Kim, J.; Tosun, A.; Kim, Y.S. *J. Cell. Biochem.* **2011**, *112*, 2179-2188.
77. Yoon, H.J.; Moon, M.E.; Park, H.S.; Im, S.Y.; Kim, Y.H. *Biochem. Biophys. Res. Commun.* **2007**, *358*, 954-959.